Ordered Stuctures of Block Copolymer/Homopolymer Mixtures. 5. Interplay of Macro- and Microphase Transitions

Satoshi Koizumi,† Hirokazu Hasegawa, and Takeji Hashimoto*

Division of Polymer Chemistry, Graduate School of Engineering, Kyoto University, Kyoto 606-01, Japan

Received May 17, 1994; Revised Manuscript Received August 4, 1994®

ABSTRACT: Self-assembly in the solution-cast films of binary mixtures of poly(styrene-*block*-isoprene) (SI) and homopolystyrene (HS) in the dry brush regime was studied by means of transmission electron microscopy (TEM) and light scattering (LS). This self-assembly involves the interplay of the macrophase and microphase transitions. In the case of a low volume fraction of SI, the macrophase separation between SI and HS first takes place via spinodal decomposition (SD) during the solvent evaporation process. This process is subsequently followed by the microphase transition, forming microdomains inside the macrodomains rich in SI. The process is eventually frozen by vitrification. The spatial concentration fluctuations developed by SD are visualized using the microdomains as a probe. In the case of the mixture with a cylinder-forming block copolymer, the following two structures were observed, depending on the solvent evaporation rate: a rapid evaporation develops the spherical microdomains of polyisoprene block chains, the centers of mass of which are dispersed in the continuous matrix of HS with the fractal-like spatial distribution; in the case of slow evaporation the self-assembled structure consists of *lenslike macrodomains*, in which cylindrical microdomains are packed hexagonally, dispersed in the continuous matrix of HS. The solution-cast film of the mixture with a lamella-forming block copolymer shows the oblate-spheroidal macrodomains, in which lamellar microdomains are packed like an *onion*, dispersed in a continuous matrix of HS.

I. Introduction

Self-organization of polymer mixtures via phase transition has been attracting many theoretical and experimental studies.[1] Especially, pattern formation in mixtures of A–B type diblock copolymers and A homopolymers involves interesting problems, because ordered structures formed in the mixtures strongly depend on the interplay of macrophase transition and microphase transition. According to our previous investigation,[2,3] we can classify A–B/A mixtures using the ratio of the degree of polymerization of A homopolymer to that of A block chains in the A–B block copolymer, r_s, defined as follows:

$$r_s = N_{A,homo}/N_{A,block} \quad (1)$$

where $N_{A,homo}$ and $N_{A,block}$ are the degrees of polymerization of the A homopolymer and A block chain, respectively.

Let us consider A–B/A mixtures such as the poly(styrene-*block*-isoprene) (SI)/homopolystyrene (HS) mixture, in a segregation regime in which neat A–B block copolymer forms lamellar microdomains in the equilibrium state. In the case of $r_s \leq 1$, it was found that A homopolymer tends to be selectively solubilized into the A-rich phase of the microdomain structure formed by the A–B block copolymer. This case was further classified into two regimes:[2,3] (i) $r_s \ll 1$, "**wet brush**" regime, and (ii) $r_s \cong 1$, "**dry brush**" regime.

This paper focuses on the mixtures satisfying $r_s \gg 1$ in which the macrophase transition between A–B block copolymer and A homopolymer dominates the microphase transition.[4,5] This is a new regime which has not been extensively studied before. In this regime, upon increasing the segregation power between components A and B, the macrophase separation between disordered A–B block copolymer and A homopolymer first takes place to induce a concentration fluctuation having a length scale (Λ_{macro}) greater than that of the microdomains. As the macrophase separation proceeds and the amplitude of the concentration fluctuations of A–B or A increases, the local concentration of A–B block copolymer in the copolymer-rich macrophases reaches the critical concentration for the microphase separation. The microphase separation starts to occur at this stage, giving rise to a characteristic microdomain spacing (Λ_{micro}). The interplay between the two kinds of phase transitions produces complex but interesting structures: coexistence of homopolymer-rich macrodomains and copolymer-rich macrodomains comprising a microdomain structure. This is a kind of **mesoscopic modulating** superstructure. The structure has dual periodicities (Λ_{micro} and Λ_{macro}) and hence may be called a **mesoscopic superlattice** structure.

In this work we used two kinds of SI; one has lamellar microdomains and the other cylindrical macrodomains in thermal equilibrium. We employed transmission electron microscopy (TEM) and light scattering (LS) to investigate the ordered structures formed in the solution-cast films. Along with these techniques we employed random phase approximation (RPA) in the analysis of thermodynamic stability for a given mixture to elucidate the mechanism of ordering processes and the interplay of macrophase and microphase transitions.

II. Experimental Methods

Two kinds of SI copolymers coded H102 (kindly supplied by Kuraray Co., Ltd.) and B1 (synthesized in this laboratory) were used in this work. Characteristics of the block copolymers are summarized in Table 1. Neat SI copolymer H102 has a microdomain morphology of alternating lamellae, while neat SI copolymer B1 has a microdomain morphology of polyisoprene (PI) cylinders in a polystyrene (PS) matrix. The homopolystyrene (HS) coded S570 (synthesized in this laboratory) was used in this work. S570 has the number-average molecular weight of 5.77×10^5 which is much larger than those of the PS block chains of H102 and B1. r_s is 11.5 and 8.5 for H102/S570 and B1/S570, respectively. The 20/80 (wt %/wt %) mixtures of H102/S570 and B1/S570 were prepared as well as the 40/60 (wt %/wt %) mixture for H102/S570. Test films of these mixtures were

* To whom correspondence should be addressed.
† Present address: Neutron Scattering Laboratory, Department of Materials Science and Engineering, Japan Atomic Energy Research Institute, Tokaimura, Ibaraki 319-11, Japan.
® Abstract published in *Advance ACS Abstracts*, September 15, 1994.

0024-9297/94/2227-6532$04.50/0

Table 1

code	M_n	M_w/M_n	wt % of PS	morphology
H102	1.0×10^5	1.10	50	lamella
B1	8.2×10^4	1.15	83	PI cylinder
S570	5.8×10^5	1.34	100	PS homo

prepared by casting from solutions in two different solvents, toluene and dichloromethane, which are both mutually good solvents for PS and PI. The casting was carried out in a vacuum oven under controlled pressure at room temperature in order to control the rate of solvent evaporation. Because of the difference in their vapor pressure, dichloromethane evaporates faster than toluene. Thus obtained as-cast films were examined by TEM and LS. For TEM observations test specimens were first stained with osmium tetraoxide (OsO_4) vapor, microtomed into ultrathin sections of ca. 50 nm thickness with an LKB 4800A Ultrotome, and subjected to the investigation under a Hitachi H-600S transmission electron microscope operated at 100 kV.

III. Experimental Results

A. TEM Observations of the H102/S570 Mixture. Figure 1 shows a transmission electron micrograph of the binary mixture of H102/S570 (40/60 wt %/wt %) cast from a 5.0 wt % toluene solution. The solvent was evaporated slowly under atmospheric pressure over 10 days. It is seen that the SI-rich macrodomains, which are not spherical but ellipsoidal, are dispersed in the matrix of HS (S570). The macrodomains rich in SI (H102) are composed of the alternating lamellae of PS and PI microdomains which correspond to the equilibrium morphology of neat H102. Small-angle X-ray scattering profiles for both H102/S570 and neat H102 show multiple-order scattering maxima with the same average lamellar spacing of 61 nm.[5] This indicates that the lamellar microdomains in the SI-rich macrophase in the H102/S570 mixture hardly solubilize HS having such a large molecular weight or a large value of r_s. It should be noted that all the macrodomains rich in SI are surrounded by a dark layer of the PI phase which implies that a monomolecular layer of H102 exists along the macrodomain interface between the HS- and SI-rich macrophases, as schematically shown in the inset at the upper right corner of Figure 1. The lamellar interfaces are forced to be curved in the ellipsoidal macrodomains rich in SI. The average diameter of the SI macrodomains is more than a few micrometers. The number of the SI lamellae in the stack is about 60 which is directly related to the diameter of the macrodomain. The grain boundary structure is observed along the long axis of the ellipsoidal macrodomain, as marked by a broken white line. It should be noted that the defects in the lamellar microdomains are more distinct nearer to the center of the macrodomain than to the periphery. Analyses of grain boundary structures for lamellar microdomains have been reported.[6,7]

Figure 2 shows a transmission electron micrograph of the binary mixture of H102/S570 (20/80 wt %/wt %) cast from a 5.0 wt % toluene solution by rapid evaporation under a moderately reduced pressure not to let it boil. It took about 20 min to evaporate the solvent from the specimen, and the evaporation rate is much faster than that under atmospheric pressure. The specimen exhibits the macrophase separation between SI (H102) and HS (S570) similar to Figure 1, but the average diameter of the dispersed macrodomains is ca. 0.5 μm, which is much smaller than that in Figure 1. Most of the macrodomains, the interfaces of which again consist of the monomolecular layers of SI, have an "*onion structure*",[8] with the exception of the domains marked by X in the figure. The shape of the macrodomains rich in SI is not so elongated as that shown in Figure 1.

Figure 3 shows a transmission electron micrograph of the same specimen shown in Figure 2, but the micrograph was taken with a much lower magnification. It appears that the spacing between the SI-rich macrodomains is quite uniform and the size distribution of the macrodomains is also narrow.

B. TEM Observations for the B1/S570 Mixture. Figure 4 shows a transmission electron micrograph of the binary mixture of B1/S570 (20/80 wt %/wt %) cast from a 5.0 wt % dichloromethane solution under a reduced pressure. The evaporation of dichloromethane took ca. 10 min, which is much faster than the evaporation of toluene under the reduced pressure. It should be noted again that neat B1 shows a microdomain structure of hexagonally packed cylinders. However, Figure 4 shows that the spherical microdomains composed of the PI block chains of SI (B1) are dispersed in the matrix composed of the PS block chains of SI and HS. The spatial distribution of the spherical microdomains is not uniform but fractal-like, exhibiting dense and dilute regions of the spheres.

Figure 5 shows a transmission electron micrograph of the B1/S570 (20/80 wt %/wt %) mixture cast from a 5.0 wt % toluene solution under atmospheric pressure. **This condition corresponds to the pattern formation under the slow solvent evaporation.** Figure 5a shows that the macrodomains rich in SI(B1) are dispersed in the matrix composed of HS (S570) and that SI forms cylindrical microdomains in the SI-rich macrodomains. In contrast to the H102/S570 mixture, no monomolecular layer of the SI block copolymer is observed at the macrodomain interfaces so that the PS microdomains composed of the PS block chains in the SI-rich macrodomain are continuous with the matrix composed of HS. It should be mentioned that these SI-rich macrodomains have a very characteristic shape; i.e., they are not spherical but *lenslike* (*truncated oblate spheroid*). It should be emphasized that the PI cylindrical microdomains in the lenslike macrodomains are not bent along the macrodomain interfaces, unlike the lamellar microdomains in H102/S570. Moreover, all PI cylinders are packed in the hexagonal lattice and highly oriented parallel to the short axis of the lenslike macrodomain. Some macrodomains marked by arrows exhibit complicated patterns of the microdomain structure. However, it was found that these patterns can be successfully reproduced by using a hexagonally-packed cylinder model with its cylindrical axis inclined with respect to the normal vector for the thin section prepared for the TEM observation. This feature will be demonstrated elsewhere[9] by computer simulation of electron microscopic images.

Parts b and c of Figure 5, respectively, show the typical top and lateral views of the lenslike macrodomains rich in SI. Figure 5b is believed to be a view obtained for the lens whose axis of the revolution, parallel to the cylinder axis, is normal to the ultrathin section, while Figure 5c is thought to be the one obtained for the lens whose axis of the revolution is parallel to the surface of the ultrathin section. The lateral dimension $l_\perp$ and the vertical dimensions $l_\parallel$ of the lenslike macrodomains are defined in Figure 5b,c. The ratio of these dimensions $l_\perp/l_\parallel$ is ca. 3.5 in the TEM image. Thus the lenslike macrodomains are the "single crystals" of the cylindrical microdomains. It should be noted that stringlike arrays of the PI spherical microdomains exist at the lateral edges of this single crystal (as shown in the portions marked A) and a small number of isolated spherical microdomains formed by SI can be

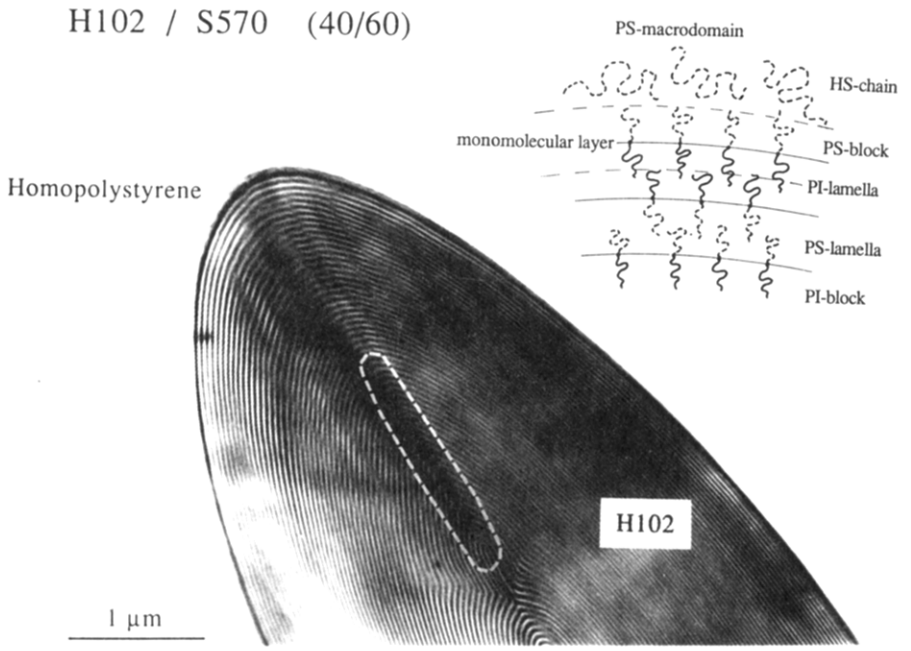

Figure 1. Transmission electron micrograph obtained from the binary mixture of H102/S570 (40/60 wt %/wt %) cast from a 5.0 wt % toluene solution with a slow rate of solvent evaporation under a normal pressure. The lamellar microdomains formed by H102 are packed like an onion ring in the SI-rich macrodomain dispersed in the matrix of S570. The inset at the upper right corner of the figure schematically shows a unimolecular layer of H102 along the microdomain interface between the HS and SI macrophases.

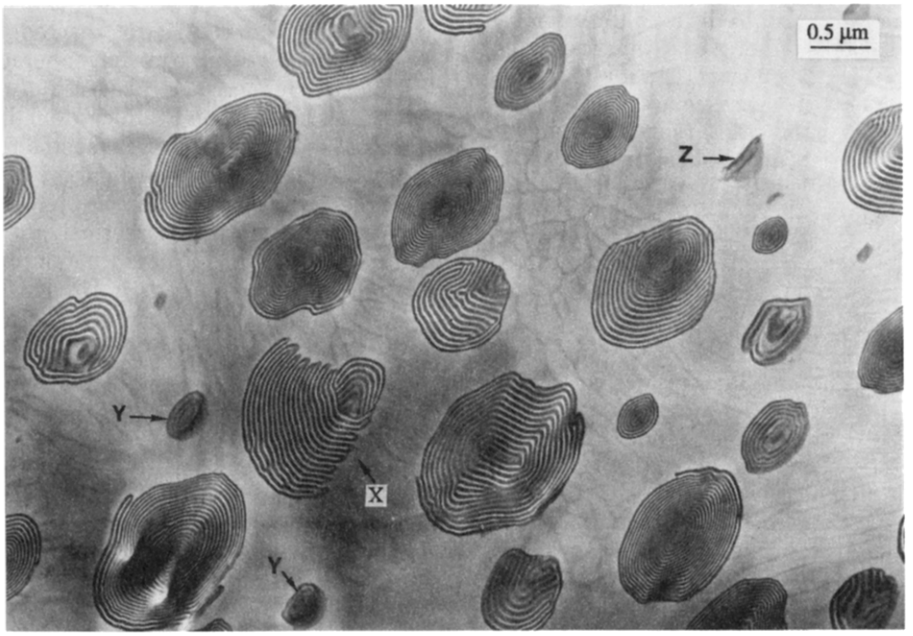

Figure 2. Transmission electron micrograph obtained from the binary mixture of H102/S570 (20/80 wt %/wt %) cast from a 5.0 wt % solution in toluene by rapid evaporation under a low pressure.

also observed in the matrix of HS. As in Figure 4, the spatial distribution of the SI-rich macrophases provides a visual probe for the concentration fluctuations of SI and HS which resulted from the macrophase separation.

C. LS Observations for the H102/S570 and B1/S570 Mixtures. Parts a and b of Figure 6 show the LS patterns obtained from as-cast films of H102/S570 (20/80 wt %/wt %) and B1/S570 (20/80 wt %/wt %) mixtures, respectively. The test specimens for LS in Figure 6a,b were the same as those investigated by TEM, corresponding to Figures 2 or 3 and 5. Figure 6a shows clearly a spinodal ring whose maximum position gives the interdomain spacing of 3.7 μm. This estimated value is consistent with the TEM observation in Figure 3. On the other hand, Figure 6b obtained from B1/S570 does not show a spinodal ring but the excess scattering which monotonously decreases with increasing scattering angle, reflecting the concentration fluctuations in the mixture.

IV. Discussion

A. Discussions for TEM Images. Under the slow evaporation process, the solution-cast films of the H102/S570 (40/60 wt %/wt %) mixture show coexistence of the macrophase composed of almost pure SI and that composed of almost pure HS, as shown in Figure 1. Moreover the SI-rich macrophase appears to show the oblate-spheroidal shape, dispersed in the matrix of HS. This shape would reflect the self-assembling process of the mixture during the solvent evaporation process.

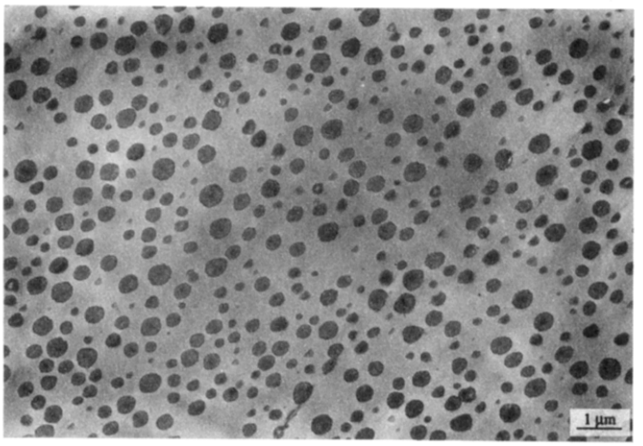

Figure 3. Transmission electron micrograph obtained from the mixture of H102/S570 (20/80 wt %/wt %) as shown in Figure 2 with a much lower magnification. The size of the SI-rich macrodomain appears to be uniform and the distribution of the interdomain distance between the macrodomains is small.

As the net polymer concentration ϕ_p of HS and SI becomes larger than the critical concentration, the mixture may become unstable for the macrophase separation, as will be discussed later in sections IV.B and IV.C. Since the solvent used is neutral to both PI and PS (and/or HS), the macrophase separation via spinodal decomposition (SD) should involve spatial concentration fluctuations of SI and HS in the medium of solvent molecules whose spatial concentration profile should be more or less uniform after the thermal averaging. As ϕ_p further increases, the concentration fluctuations between the SI-rich solution and the HS-rich solution further increase in terms of both the amplitude of the fluctuations and the spatial scale over which the concentration fluctuations persist. This ordering process may eventually form droplets of the disordered SI solution in the matrix of the HS solution. The droplets are expected to be spherical in order to minimize the interfacial free energy.

As ϕ_p further increases, the disordered SI solution in the droplets can now undergo the microphase separation, forming the lamellar microdomains swollen with solvent. Since bending of the lamellar interfaces costs the elastic free energy in packing polymer coils in the microdomains, the interfaces tend not to be bent as much as possible. This may explain the deformation of the droplets into the oblate-spheroidal shape whose axis of revolution is parallel to the average orientation of the normal vectors of the lamellar interfaces.

The grain boundary defects in which the lamellae with different orientations meet each other are rich in the center of the SI microdomains. This may imply that the microphase separation progresses from the periphery of the droplets toward their centers. Thus the packing of lamellae becomes onionlike. This particular growth of the lamellae induced by the microphase separation may be driven by the following two physical factors: (i) surface-induced ordering and (ii) a space-dependent driving force for the microphase separation. As for the former (i), the outer surface of the droplets composed of the disordered SI solution is in contact with the HS solution. Therefore, even when the SI solution is in a disordered state, the outer surface of the SI droplets may be enriched by the PS segments of the SI block copolymers in order to minimize the surface free energy.[16] As the segregation power increases, it is naturally expected for the ordering to progress from their outer edges toward their centers. As for the latter (ii), there is a spatial concentration gradient of SI, $\phi_{block}(r)$, across the SI droplets, which may cause the local thermodynamic instability for the microphase separation for the single phase mixture of HS and disordered SI to depend on position r. If this is the case, the driving force for the microphase separation should also depend on r. Furthermore, it is possible that the driving force is the largest in the periphery of the droplets and decreases toward their centers, as will be discussed later in section IV.C.

A rapid solvent evaporation of the mixture of H102/S570 (20/80 wt %/wt %) results in the SI-rich macrodomains having a relatively uniform size and spacing, as highlighted by the TEM in Figure 3 and the LS pattern in Figure 6a. This unique pattern is considered again to reflect the macrophase separation via SD and a subsequent coarsening process. At a certain stage of the solvent evaporation process, SD takes place in the system and it generates a bicontinuous periodic domain structure which is composed of the phase rich in the SI solution and that rich in the HS solution. As the domain grows, a minority phase (the SI-rich solution phase) cannot maintain the continuous structure and results in formation of the droplets (percolation-to-cluster transition[10]). The size and the spatial distribution of the droplets should be relatively uniform, because the droplets originate from the periodic domain structures generated by SD.

As ϕ_p further increases, the microphase separation starts to occur in the SI-rich droplets, resulting in formation of the lamellar microdomains inside the droplets. However, as an average droplet size is small, the number of lamellae formed in it is also small compared with that shown in Figure 1. The aspect ratio of the deformed macrodomains rich in SI seems to be coupled with the number of lamellae inside the domains; the aspect ratio is small for the small domains with the small number of lamellae (Figure 2) compared with that for the large domains with the large number of lamellae (Figure 1). At the time when the microphase separation starts to occur, the small SI-rich droplets formed in the rapid solvent evaporation process may contain a greater fraction of HS than the large SI-rich droplets formed in the slow solvent evaporation process. An excess amount of HS, which may tend to be segregated out from the droplets during the course of the microphase separation, may happen to be trapped between the PI lamellae in the case of the rapid solvent evaporation process. The trapped HS are then expected to cause the formation of the vesicular macrodomain structures composed of lamellae,[5] as marked by X, Y, and Z in Figure 2.

We now discuss the TEM images obtained from B1/S570 (20/80 wt %/wt %) under different solvent evaporation rates: Figure 4 (obtained by the rapid evaporation) vs Figure 5 (obtained by the slow evaporation). It should be noted here again that neat B1 has PI cylinders dispersed in the PS matrix in equilibrium. The experimental results would again indicate that the macrophase separation occurs prior to the microphase separation. It is expected in the rapid solvent evaporation that the microphase separation starts to occur in the SI-rich macrodomains containing a larger fraction of HS, compared with the case of the slow evaporation. During the microphase separation process, some amount of HS may tend to be segregated out from the SI-rich domains, but the amount segregated is less in the fast solvent evaporation. Hence a greater amount of HS tends to be trapped in the region rich in SI where the microphase transition occurs.

Thus the fast solvent evaporation develops the spherical microdomains of the PI block chains dispersed in the PS

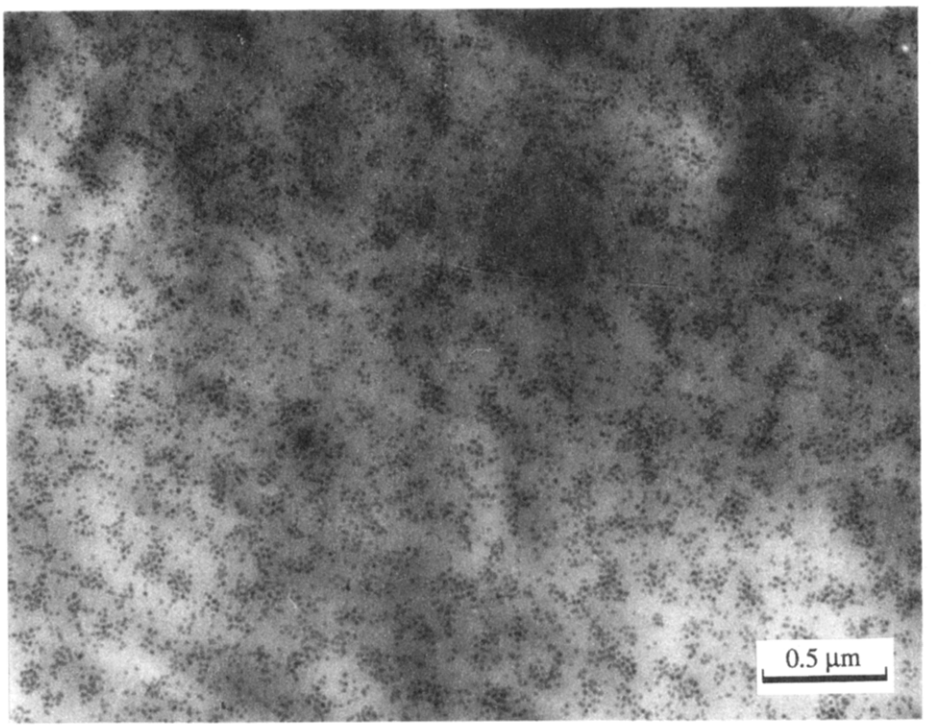

Figure 4. Transmission electron micrograph obtained from the mixture of B1/S570 (20/80 wt %/wt %) cast from the 5.0 wt % dichloromethane solution under a low pressure. It shows a fractal-like spatial distribution of the spherical microdomains. Note that the neat B1 itself shows the cylindrical microdomains.

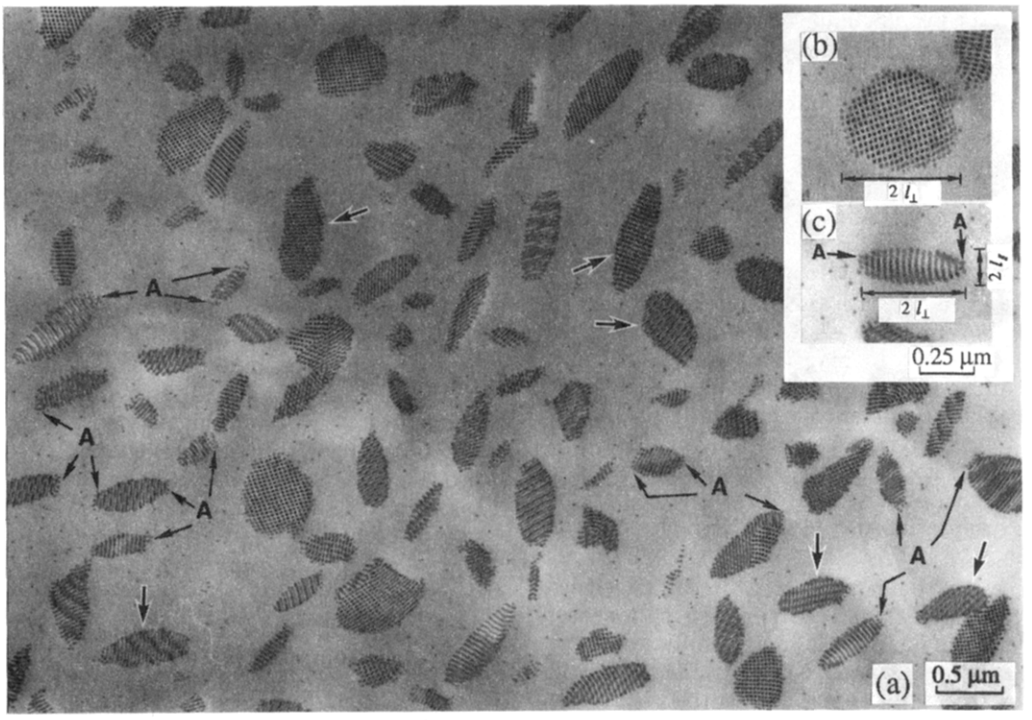

Figure 5. (a) Transmission electron micrograph obtained from the mixture of B1/S570 (20/80 wt %/wt %) cast from the 5.0 wt % toluene solution under a normal pressure. The *lenslike* macrodomains rich in B1, in which the PI cylinders are packed hexagonally, are dispersed in the matrix of S570. (b) and (c) show the typical top and lateral views of the lenslike macrodomains in which the lateral and vertical dimensions, $l_\perp$ and $l_\parallel$, are defined.

block chains and HS in the SI-rich macrodomains (Figure 4), generating clusters of the spherical microdomains distributed in the matrix composed of HS. Here the PS block chains emanating from the PI spheres must be swollen with HS to some extent, because the spherical microdomains exist instead of the cylindrical microdomains. The nonuniform, fractal-like, spatial distribution of the spherical microdomains would reflect and visualize the concentration fluctuations of SI and HS in the SD process at the instance when the microphase separation occurs.

On the other hand in the case of the slow solvent evaporation, the microphase separation is expected to occur in the later stage of SD, so that the SI-rich macrodomains have larger sizes and contain a smaller amount of HS, compared with the case of the fast solvent evaporation. We therefore expect that the hexagonally-packed cylindrical microdomains of the PI block chains

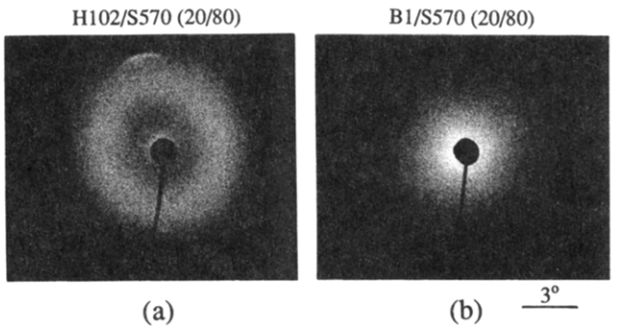

Figure 6. LS patterns obtained from as-cast films of the H102/S570 and the B1/S570 mixtures, respectively. Part a shows clearly the spinodal ring whose maximum position corresponds to the interdomain spacing of 3.7 μm. Part b obtained from B1/S570 does not show the spinodal ring but the excess scattering which monotonically decreases with increasing scattering angle.

are formed in the matrix composed mostly of the PS block chains and that the macrophases composed of the cylinders are larger than those of the spheres formed by the rapid solvent evaporation.

The macrodomains containing the PI cylinders are unique in shape. The qualitative features of the lenslike shape observed in the TEM images are schematically illustrated in Figure 7 where the lenses have an average shape as shown in part a, **a truncated oblate spheroid** having the axis of revolution along the z-axis and the characteristic lengths $l_\parallel$ and $l_\perp$ parallel and perpendicular to the z-axis, respectively. The cylinders are packed in a hexagonal lattice in the plane perpendicular to the z-axis, as shown in part b, and the cylinder axis is parallel to the z-axis, as shown in part c. The shape of the lens is characterized by the aspect ratio $l_\perp/l_\parallel \cong 3.5$ (part c).

The lenses are not covered with the SI monomolecular layer as in the macrodomains containing lamellar microdomains (as illustrated in the inset of Figure 1); i.e., the molecular structure of the macrodomain interface between the lens and the HS matrix is different from that between the lamellar macrodomains and the HS matrix. The difference is schematically illustrated in parts d and e in Figure 7. The end surface of the lens which is nearly normal to the z-axis may have a surface free energy γ_e different from the surface free energy γ_s of the lateral surface of the lens parallel to the z-axis (see part d and e, respectively). The difference may originate from a difference in packing and molecular conformation of the block chains at the lateral interface and the end interface of the cylindrical microdomains. The difference in the surface free energy γ_e and γ_s may provide a possible interpretation of the lenslike macrodomains.

A close observation of the lenses would reveal the existence of an array of the PI spheres parallel to their z-axes at each lateral edge of the lenses for most of the lenses whose z-axes lie parallel to the plane of the TEM image or the surface of the ultrathin section for the TEM observation (see portions of the TEM image marked by A in Figures 5 and 7c). This may be related to the Rayleigh–Tomotika instability[11] of an isolated thread of liquid in the matrix of another liquid. The cylindrical microdomains of the block copolymers may be stable when they are surrounded by the neighboring cylindrical microdomains. However, when they are isolated, they may become unstable and will be broken into an array of the PI spheres, as in the case of the viscous thread. Similarly, the cylinders located at the lateral edges of the lenses may be subjected to the instability as they are exposed to the interaction with the matrix. The instability of the

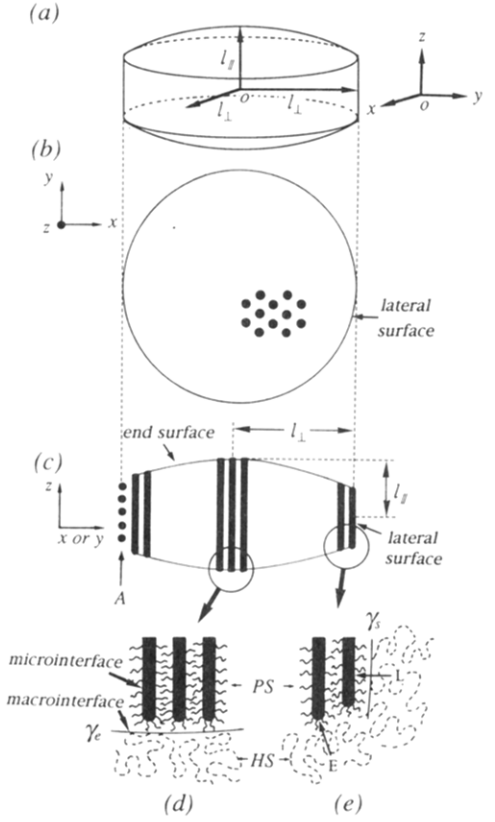

Figure 7. Schematic diagrams showing the lenslike macrodomain observed in the binary mixture of B1/S570 (20/80 wt %/wt %). (a) The truncated oblate spheroid has the axis of revolution along the z-axis and the characteristic lengths $l_\parallel$ and $l_\perp$ parallel and perpendicular to the z-axis, respectively. (b) The cylinders inside the lenslike domains are packed in a hexagonal lattice in the plane perpendicular to the z-axis and (c) the cylinder axis is parallel to the z-axis. An array of the spherical microdomains parallel to the z-axis can be observed at the lateral edge of the lenslike macrodomain marked A. (d) and (e) show a difference in packing and molecular conformation of the block chains at the lateral interface L and the end interface E of the cylindrical microdomains. The macrointerface and the microinterface are also defined.

cylinders is quite a contrast to the stability of the lamellae: the lamellae are stable even when they are well separated by HS, forming the vesicles.[5]

In the TEM images as shown in Figure 5b in which the z-axis of the lens is oriented normal to the ultrathin section, the outermost microdomains (cylindrical or spherical microdomains) in the lens have a weaker contrast than those inside. The observation is consistent with our interpretation that the macrodomains are lenslike. Here it should be noted that the thickness of the ultrathin section (ca. 50 nm) is much thinner than the average dimension of $l_\parallel$ (ca. 0.2 μm), so that the curvature of the end surface of the lens cannot be seen through the spatial distribution in the contrast of the dark circles. The weaker contrast of the dark circles in the outermost area of the lens therefore reflects the existence of the PI spheres rather than PI cylinders.

B. Interplay of Macro- and Microphase Separations. For the binary mixtures of SI and HS, the self-assembled structure is governed by the interplay of the macrophase transition and the microphase transition.[1,4,12] In the particular case of $r_s \gg 1$, the spinodal decomposition (SD) between SI and HS may be initiated at first with an increase in polymer concentration during the solvent evaporation process. As the amplitude of the concentra-

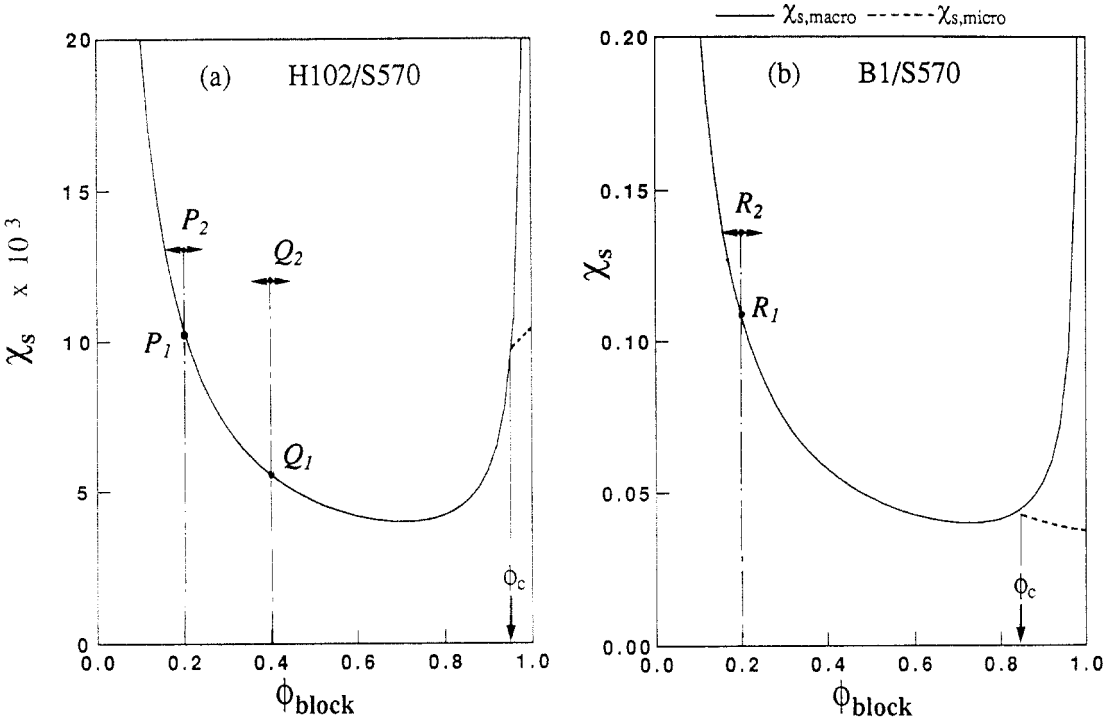

Figure 8. Phase diagrams calculated by RPA, showing the spinodal lines for macrophase (solid lines) and microphase transitions (broken lines) for the binary mixtures (a) H102/S570 and (b) B1/S570. Both mixtures have a chance to encounter the microphase transition first within the compositional range $\phi_c < \phi_{block}$.

tion fluctuation increases in the course of SD, the SI-rich macrodomains reach the critical concentration ϕ_c where SI becomes unstable for the microphase transition and undergoes the microphase separation. The final structure crucially depends on the concentration fluctuations at the time when the microphase separation takes place. Thus the solution-cast films of the mixtures may exhibit the structure containing dual modes of the concentration fluctuations, one having a characteristic length of 1000 Å or larger which is developed by the macrophase separation via SD and the other having the characteristic length scale of about 100 Å which is developed by the microphase separation. In order to understand the final structure, it is crucial to investigate in-situ the ordering process. However, the real ordering process is complicated because the ordering process occurs athermally; i.e., the polymer concentrations and hence the segregation power change with time during the ordering processes.

C. Qualitative Interpretation Based upon RPA. In order to investigate the self-assembly and the ordering process of the mixture of SI and HS, the spinodal lines or the thermodynamic stability limits for the macro- and microphase transitions were calculated in the context of RPA. The detailed calculations were described in the previous papers.[4,13,14] Parts a and b of Figure 8 show the calculated spinodal curves for the mixtures of H102/S570 and B1/S570, respectively. The interaction parameters at the spinodal points χ_s ($\chi_{s,macro}$ and $\chi_{s,micro}$) for the macrophase and the microphase transitions are plotted against the volume fraction of the block copolymers in the mixtures, ϕ_{block}. The solid curves denote χ_s for the macrophase transition $\chi_{s,macro}$ at which the Fourier mode of the concentration fluctuation with the wavenumber $q = 0$ becomes unstable, and the broken curves, χ_s for the microphase transition $\chi_{s,micro}$ at which the Fourier mode having the wavenumber $q = q_m \cong 1/R_g$ becomes unstable. Here R_g is the radius of gyration of a given block copolymer. Both the H102/S570 and B1/S570 mixtures have a chance to encounter at first the microphase transition within the compositional range $\phi_c < \phi_{block}$ with increasing effective segmental interaction χ between PI and PS (or HS). Here ϕ_c is the Lifschitz point where the system becomes unstable for both the macro- and microphase transitions.

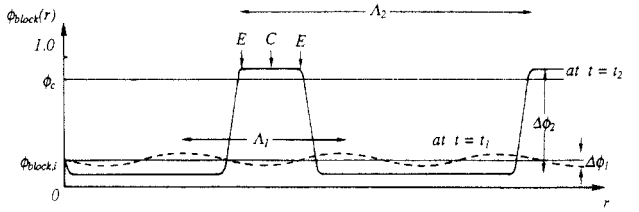

Figure 9. Schematic diagrams showing the concentration variation at the times t_1 and t_2, which correspond to an early stage and a late stage, respectively, of the spinodal decomposition between SI and HS.

As χ increases, each mixture studied here reaches the spinodal point for the macrophase transition at P_1, Q_1, or R_1 and hence undergoes the macrophase separation via SD. If the systems are quenched inside the spinodal line, e.g., at point P_2, Q_2, or R_2 and kept there, the amplitude $\Delta\phi(t)$ and the wavelength $\Lambda(t)$ of the dominant modes of the concentration fluctuations grow with time, generating regions rich in SI and those rich in HS.[1] Figure 9 schematically represents the dominant modes of the concentration fluctuations of SI at two representative times t_1 (broken line) and t_2 (solid line) ($t_1 < t_2$). A difference of the block copolymer composition ϕ_{block} between the two domains $\Delta\phi(t)$ increases with time from $\Delta\phi_1$ to $\Delta\phi_2$. As the fluctuations increase, in terms of $\Lambda(t)$ and $\Delta\phi(t)$, the SI-rich domains start to have the local composition $\phi_{block}(r)$ greater than ϕ_c. The microphase separation can start to occur in these SI-rich regions satisfying $\phi_{block}(r) \geq \phi_c$. The microdomain morphology developed in the SI-rich macrodomains should depend on ϕ_c, as it determines the local concentration of SI/HS at the time when the microphase separation occurs. When the microphase separation occurs, HS may be segregated out or included in the microdomains, depending on the relative rate of the translational diffusion of HS and the growth rate of the microdomain. The segregation also affects the morphology

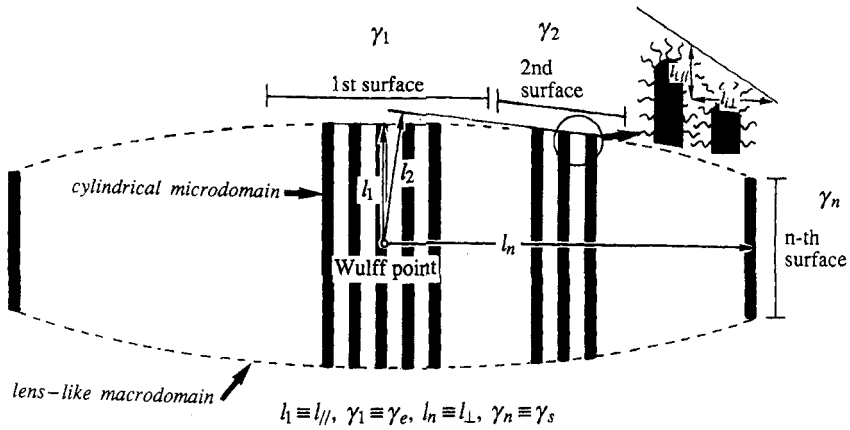

Figure 10. Polygon model to explain the lenslike macrodomain comprising the cylindrical microdomains on the basis of the Wulff theory.[15]

of the microdomain in the SI-rich domain. These effects on morphology are highlighted in the TEM images obtained for the solution-cast films of the B1/S570 mixtures prepared by the different solvent evaporation rates.

It is worthwhile to note that $\chi_{s,micro}$ increases with ϕ_{block} for the H102/S570 mixtures but decreases for the B1/S570 mixtures. This means that the H102/S570 mixtures become increasingly unstable for the microphase transition with the increasing fraction of HS (S570), while the B1/S570 mixtures become more stable with the increasing fraction HS. Let us consider the mixture of H102/S570 at time t_2, in which $\phi_{block}(r)$ in the SI-rich regions is greater than the critical composition ϕ_c but the block copolymers are still in the disordered state. There is a concentration variation of SI in the SI-rich macrodomains, as described schematically by the solid line in Figure 9.

Now we apply the stability analysis by RPA (shown in Figure 8) to the local area inside the SI-rich macrodomains where ϕ_{block} in the center of the domain C is larger than in the periphery E. It can be noted that the mixture H102/S570 in the regions E near the interface of the macrodomains is more unstable than those C near the center of the macrodomains, while the mixture B1/S570 in the regions C near the center of the macrodomains is more unstable than those E near the interface of the macrodomains. It may be reasonable to predict that the microphase separation will start from the most unstable parts of the SI-rich macrodomains at the time t_2 and the orientation of the microdomain inside the SI-rich domain will be governed by the microdomains first formed. If this is the case, the microphase separation may proceed from the periphery E to the center C of the droplets for the H102/S570 mixtures. On the other hand, for the B1/S570 mixture, the microphase separation may start from the center C of the droplets and proceed toward the periphery E. That may be why the monomolecular layer covering the SI-rich macrodomains was not observed at the macrodomain interface for the mixture of B1/S570. The orientation of cylinders inside the SI-rich domain may be controlled by the first cylinder formed near the center of the macrodomains.

D. Equilibrium Shape of the Macrophase Rich in Block Copolymers. In the strong segregation limit, the shape of the SI-rich macrodomains may be determined by thermodynamic requirement to minimize the total free energy. The free energy may be composed of two major terms, i.e., bulk free energy originating from microdomains formed inside and surface free energy at the macrodomain interface.

In the case of H102/S570 mixtures, the block copolymer H102 has a volume fraction of PS/PI nearly equal to 50/50 and favors a flat interface because of the cost of the elastic free energy for bending the lamellar interface which may be proportional to a number of the stacked lamellae. The aspect ratio is expected to increase with the increasing size, i.e., increasing number of incorporated lamellae. Furthermore for the H102/S570 mixtures, an anisotropy of the surface free energy is not expected because the SI-rich macrodomains are uniformly surrounded by monomolecular layer which realizes a contact between HS and the PS block chains. Thus the elastic free energy associated with curvature of the lamellar interfaces or bending deformation of lamellae in the SI-rich macrodomains may play an important role in controlling the shape of the macrodomains.

In the lenslike macrodomains observed in the B1/S570 mixture, the PI cylindrical microdomains are found to be packed hexagonally without bending. However, the lenslike macrodomains have two kinds of interfaces between HS and the PS block chains, i.e., the end and lateral surfaces (see Figure 7d,e). According to Wulff's theory,[15] we can find the thermodynamic relation as follows:

$$\gamma_i/l_i = \text{constant} \qquad i = 1, 2, ..., n \tag{2}$$

where γ_i is the surface tension of ith surface and l_i is the distance from the Wulff point to the ith surface. In the case of the lenslike macrodomain, the Wulff point corresponds to the center of the lenslike macrodomain as illustrated in Figure 10. Here it should be noted that l_1 and l_n correspond to the lateral and vertical dimensions (defined $l_{//}$ and $l_\perp$ in Figure 7) for the lenslike macrodomain, respectively. The lenslike macrodomain is a polygon composed of multisurfaces having different local orientations. The orientation of the ith surface is determined by the ratio of $l_{i//}$ and $l_{i\perp}$, i.e., the lengths of the lateral and end surface facing the matrix of HS (see the inset of Figure 10). The surface characterized by a different slope may have a different surface tension. However, in the case of the lenslike macrodomain, it will be expected that the surface tensions from 1st to $(n-1)$th are almost equal to each other ($\gamma_e \equiv \gamma_1 \cong \gamma_2 \cong ... \cong \gamma_{n-1}$) and that the surface tension of the lateral surface $\gamma_n \equiv \gamma_s$ is quite different from the others ($\gamma_s > \gamma_e$).

According to the TEM observation, the lenslike single crystal has the aspect ratio $l_\perp/l_{//} \cong 3.5$ which is directly

related to the ratio of the interfacial tension γ_s/γ_e.

$$\gamma_s/\gamma_e \cong 3.5 \quad (3)$$

It may be surprising at first glance that the interfacial tension of the lateral surface of the lenslike macrodomain is larger than that of the end surface. However this may seem to be reasonable in view of the free energy of the "**macrointerface**" made by packing between the PS block chains and the HS chains. As illustrated in Figure 7e, the "**microinterface E**" at the end of the PI cylinders has a mean curvature bigger than that of the microinterface L at the side of the PI cylinders. This will make a space for packing the PS and HS chains at the end surface bigger than that at the later surface, possibly making the end surface free energy γ_e lower than the lateral surface free energy γ_s.

V. Conclusion

Self-assembly involved in the solvent-cast films of the binary mixtures of poly(styrene-*block*-isoprene) (SI) copolymer and homopolystyrene (HS) satisfying $r_s \gg 1$ was studied by TEM and LS. The concentration fluctuations developed by spinodal decomposition (SD) between SI and HS were visualized using the microdomains as a probe. It was revealed that the ordered structures in the films are determined by the interplay of macrophase and microphase transitions. In the case of fast solvent evaporation, the concentration fluctuations were frozen at a relatively early stage of SD: in the case of the B1/S570 (20/80 wt %/wt %) mixture, the remaining HS in the SI-rich macrodomains causes the morphological transition of the microdomain from PI cylinders to PI spheres, while in the case of the H102/S570 (20/80 wt %/wt %) mixture, the SI-rich macrodomains comprising the lamellar microdomains have a narrow size distribution and are uniformly dispersed in the matrix of HS. The spatial distribution of PI spheres in the former mixture is not uniform but fractal-like. When the rate of solvent evaporation is low, the B1/S570 mixtures show the truncated oblate-spheroidal (lenslike) macrodomains rich in SI dispersed in the matrix of HS. In the case of the H102/S570 (20/80 and 40/60 wt %/wt %) mixtures, the macrodomains comprise the lamellar microdomains which are packed like an onion structure, while in the case of the B1/S570 (20/80 wt %/wt %) mixture the macrodomains comprise the cylindrical microdomains which are packed hexagonally with their axes parallel to the short axis of the lenslike macrodomain.

Acknowledgment. We thank Prof. T. Ohta for useful discussions. This work was partially supported by a Grant-in-Aid for Scientific Research from the Ministry of Education, Science, and Culture, Japan (05650673).

References and Notes

(1) See for example: Hashimoto, T. In *Structure and Property of Polymers*; Cahn, R. W., Haasen, P., Kramer, E. J., Eds.; Materials Science and Technology, Vol. 12; VCH: Weinheim, 1993; p 251.
(2) Hashimoto, T.; Tanaka, H.; Hasegawa, H. *Macromolecules* **1990**, *23*, 4378.
(3) Tanaka, H.; Hasegawa, H.; Hashimoto, T. *Macromolecules* **1991**, *24*, 240.
(4) Tanaka, H.; Hashimoto, T. *Polym. Commun.* **1988**, *29*, 212.
(5) Koizumi, S.; Hasegawa, H.; Hashimoto, T. *Makromol. Chem., Macromol. Symp.* **1992**, *62*, 75.
(6) Nishikawa, Y.; Kawada, H.; Hasegawa, H.; Hashimoto, T. *Acta Polym.* **1993**, *4*, 247.
(7) Gido, S. P.; Gunther, J.; Thomas, E. L.; Hoffman, D. *Macromolecules* **1993**, *26*, 2636.
(8) Riess, G.; Schlienger, M.; Marti, S. *J. Macromol. Sci.—Phys.* **1980**, *B17*, 355. Gebizlioglu, O. S.; Argon, A. S.; Cohen, R. E. *Polymer* **1985**, *26*, 519.
(9) Nishikawa, Y.; Hasegawa, H.; Hashimoto, T. To be submitted for publication.
(10) Hashimoto, T. In *Progres in Pacific Polymer Science 2*; Imanishi, Y., Ed.; Springer: Berlin, 1992; p 175. Hashimoto, T.; Sasaki, K.; Kawai, H. *Macromolecules* **1984**, *17*, 2812. Hashimoto, T.; Takenaka, M.; Izumitani, T. *J. Chem. Phys.* **1992**, *97*, 679.
(11) Rayleigh, L. *Philos. Mag.* **1892**, *34*, 145. Tomotika, S. *Proc. R. Soc. London, Ser A* **1935**, *150*, 322.
(12) Hashimoto, T.; Tanaka, H.; Hasegawa, H. In *Molecular Conformation and Dynamics of Macromolecules in Condensed Systems*; Nagasawa, M., Ed.: Elsevier: Amsterdam, 1988; p 257.
(13) Leibler, L. *Macromolecules* **1980**, *13*, 1602.
(14) Leibler, L.; Benoit, H. *Polymer* **1981**, *22*, 195.
(15) Wulff, G. Z. *Krist.* **1901**, *34*, 449. Wulff, G. Z. In *Crystal Form and Structure*; Schneer, C. J., Ed.; Domden Hutchinson and Ross, Inc.: 1977; p 43.
(16) Fredrickson, G. H. *Macromolecules* **1987**, *20*, 2535.